

SEARCH FOR A KEYWORD

MOST VIEWED POSTS

Medium-density fiberboard and edge-glued panel after edge milling – surface waviness after machining with different parameters measured by contact and contactless method

Moisture at contacts of timber-concrete element

Study on propagation law of acoustic emission signals on anisotropic wood surface

Comparative proteomic analysis of the thick-walled ray formation process of *haloxylon ammodendron* in the gurbantunggut desert, China

Preparation, chemical constituents and antimicrobial activity of pyrogallous acids from *salix psammophila* branches

WOOD RESEARCH VOLUME 69, NUMBER 4, 2024

JÁN KANÓCZ, VIKTOR KARLA, MIHAL TOMKO, TOMÁŠ BAROŠ, AND VIKTÓRIA BAJZECEROVÁ

DESIGN AND ANALYSES OF HYBRID FACADE PANELS CREATED WITH TRANSPARENT WOOD BIO-COMPOSITES

The paper presents the initial results of research focused on the possibilities of using transparent wood for building envelope structural elements in architecture. Some theoretical analyses of the hybrid envelope panels made with different types of transparent wood were carried out. The aim of the study was to assess static and hygrothermal behaviour of such panels. The panels were considered to be two layers of transparent wood bio-composites each 10 mm thick glued to an oak timber frame with only plain air as insulator in the panel. Because only small samples of transparent wood were produced so far, it was considered that mechanical properties of small samples would be retained in large ones as well.

WOOD RESEARCH VOLUME 69, NUMBER 4, 2024

YOSAFAT AJI PRANATA AND BAMBANG SURYOATMONO

EXPERIMENTAL STUDY ON FLEXURAL BEHAVIOR OF RED MERANTI (SHOREA SPP.) GLULAM BEAM OF VARIOUS NUMBER OF LAMINAE

This research aims to study flexural behavior of Red Meranti (*Shorea spp.*) glulam beam of various number of laminae by carrying out testing beams made from four, six, and eight laminae. Four points bending test method according to ASTM 198-22 was applied. The research results show that glulam composed of a smaller number of laminae reaches a smaller flexural rigidity. The empirical equations for flexural strength ratio and modulus of rupture ratio, and the trend of flexural rigidity between glulam and solid proposed in this study can be used in designing the flexural members of timber buildings, timber bridges, and in calculating the deflection of timber beams.

WOOD RESEARCH VOLUME 69, NUMBER 4, 2024

MONIKA STANKOVSKÁ, JURAJ KRÍŠTA, ŠTEFAN BOHÁČEK, ALBERT RUSS, AND ANDREJ PAŽITNÝ

COMPARISON OF TWO METHOD FOR ISOLATION OF FIBRILLATED CELLULOSE FROM LIGNOCELLULOSIC BIOMASS

Fibrillated cellulose from distillery refuse based on maize starch was prepared by two different procedures. The effect of sonification was evaluated at acid-alkali extraction as well as the type of used acid. The results from the alkali-acid procedure were compared with those obtained by method of steam explosion at different temperatures. The acid-alkali method brings a better result regarding degradation of hemicellulose and lignin as well as cellulose. Lignin/hemicellulose were only released from lignocellulose network using steam explosion at 120-180°C. At higher temperature, the results were comparable with those obtained by acid-alkali method. Similarly pore size distribution of filter paper decreased more significantly when fibrillated cellulose from acid-alkali treatment was applied. After steam explosion, higher extend of longer still fibres remains.

WOOD RESEARCH VOLUME 69, NUMBER 4, 2024

TOMÁŠ MELICHAR, SILVESTR VASAS, JIŘÍ BYDŽOVSKÝ, ŠÁRKA KEPRDOVÁ, AMOS DUFKA, AND IVETA NOVAKOVA

INFLUENCE OF PARTICULATE MIXTURE CONTAINING STABILISED WOOD ON LONG-TERM BEHAVIOUR OF WOOD-CEMENT COMPOSITES. CASE STUDY

This paper presents research on the changes in the properties of cement-bonded particleboard modified with particulate mixture (PM). PM replaced 4% of the binder (cement) and 4% of the filler (spruce chips). The cement-bonded particleboards were tested for physical (bulk density, swelling, linear expansion due to relative humidity changes) and mechanical properties (modulus of rupture and modulus of elasticity). Development of phase composition and microstructure by XRD and SEM were also analysed. The long-term behaviour of wood-cement composites was studied over a period of 2 years. The physical, mechanical properties and microstructure of the modified particleboards were compared with commercially produced cement-bonded particleboards from CIDEM Hranice, Inc. There is no intentional change in properties when using PM compared to the reference boards and the values reached the EN 634-2: 2007.

WOOD RESEARCH VOLUME 69, NUMBER 4, 2024

LOYA JAMALIRAD AND SAEED NAROUIE

LIGNOCELLULOSIC WASTE OF FURFURAL PRODUCTION FROM BAGASSE AS NON-FOOD FILLER AND SUBSTITUTE FOR UF RESIN IN PLYWOOD MANUFACTURE

The effect of lignocellulosic waste from furfural production of bagasse (LWFPB) as non-food filler for urea-formaldehyde resin (UF) and also substitute a part of UF resin in plywood manufacture was evaluated. LWFPB was used at four levels of 0, 10, 20 and 30% as filler and was replaced with UF resin at three levels of 0, 10 and 20%. Then the physical and mechanical properties of the plywood samples were measured. Results showed that the mechanical and physical properties of plywood were increased compared to the control (with wheat flour filler) when UF resin was used with LWFPB filler. Higher shear strength, MOR and MOE were associated with the use of 30% LWFPB. Besides that, the addition of LWFPB instead of UF resin reduced the mechanical and physical properties of plywood to some extent, but compared to control sample, the best results were obtained with the addition of 10% LWFPB.

WOOD RESEARCH VOLUME 69, NUMBER 4, 2024

RUI JIANG, YUANFEI XU, XUEJIAN YANG, LEI ZHANG, ZHENYU FAN, XIAOYAN GUO, FENG XIAO, LIZHI ZHU, AND BINGQIN SUN

THE EFFECT OF COLORANTS ON THE DEGRADATION PERFORMANCE OF WOOD PLASTIC COMPOSITES

The degradation performance of the colorful wood flour/poly (β -hydroxybutyrate valerate) composites (CWPHBVs) in natural outdoor landfill was investigated by some physical, analytical, and microscopic tests. The mass loss rate of the CWPHBVs within 80 days of degradation shows a growth trend and the mass loss rate decreases by more than 20%. With the increase of degradation time, the bending strength of the CWPHBVs continues to decline, the elastic modulus of the CWPHBVs shows a logarithmic decline trend. After 30 days, the bending strength of the CWPHBVs decreases over 60% and tend to be stable. The colorant has a certain inhibitory effect on the degradation. However, with the shedding of the colorant, the effect of the colorant on the degradation is gradually weakened. The addition of colorants reduces the decomposition rate of PHBV and improves the thermal stability of poplar fibers. However, after 20 days, this effect almost disappears.

WOOD RESEARCH VOLUME 69, NUMBER 4, 2024

ALBERT RUSS, ANDREJ PAŽITNÝ, JURAJ KRÍŠTA, EMMA WESZELOVSKÁ, AND VLADIMÍR IHNÁT

ENZYMATIC HYDROLYSIS OF STEAM EXPLODED STRAW WITH THE ADDITION OF ACETIC ACID

The effect of steam explosion on the enzymatic hydrolysis of straw was investigated in the presence of 5, 10, 15 and 20% wt. addition of acetic acid. Analysis was performed at temperatures of 160, 170, 180, 190, 200 and 210°C. The concentration of monosaccharides obtained after enzymatic hydrolysis was considered the main indicator of the increased availability of cellulose due to their release into the solution. The results indicate that the addition of acetic acid increases the concentration of monosaccharides, but only at lower temperatures. The temperature of 180°C corresponded to the most effective pretreatment by steam explosion in the presence of acetic acid with the highest concentration of 10%, which corresponds to the conversion of polysaccharides to monosaccharides of 74.78%. At high temperatures above 200°C, the addition of acetic acid results in a decrease in the concentration of monosaccharides due to the high severity factor in the range of 3.94 – 4.24.

WOOD RESEARCH VOLUME 69, NUMBER 4, 2024

THE ATTENUATION CHARACTERISTICS OF DIFFERENT FREQUENCY COMPONENTS OF ACOUSTIC EMISSION SIGNAL DURING PROPAGATION IN ELM AND PINE WOOD

In order to gain a deeper understanding of the attenuation characteristics of different frequency components of acoustic emission signal when propagating in wood, this research conduct pencil lead fracture experiments on the surface of elm and pine specimen. Original AE signals acquired by different sensors are decomposed using 5-level wavelet transform, the attenuation characteristics of different frequency components are studied, and the acoustic emission source is located according to the energy of different frequency components. The results indicate that the propagation distance is the main factor affecting the attenuation of AE signals. The longer the propagation distance, the greater the degree of attenuation. The attenuation characteristics of high-frequency components of acoustic emission signals deviate from the ideal attenuation model after the propagation distance greater than 10 cm. The higher the frequency components of acoustic emission signals, the faster they attenuate when propagation in elm and pine specimen.

WOOD RESEARCH VOLUME 69, NUMBER 4, 2024
HARUNA SEIDU, RÓBERT NÉMETH, AND FRANCIS WILSON OWUSU

MECHANICAL STRENGTH CHARACTERIZATION OF THREE LESSER-UTILISED TIMBER SPECIES IN GHANA

This study investigates the mechanical properties of three lesser-utilized timber species in Ghana: *Bligia sapida*, *Gilbertiodendron limba*, and *Lannea welwitschii*. Despite their potential, these species are underexplored compared to widely used commercial timbers. Six trees, two from each species, were tested for properties such as modulus of elasticity (MOE), modulus of rupture (MOR), compressive strength, shear strength, hardness, and density. Results indicate that *Bligia sapida* has superior mechanical properties, placing it in the D50 strength class, suitable for high-resistance structural applications. *Gilbertiodendron limba* and *Lannea welwitschii* are categorized under the D40 strength class, appropriate for moderate load-bearing uses. This research demonstrates that lesser-utilized species can serve as viable alternatives to traditional timbers, potentially reducing pressure on overexploited species. By promoting their use, the study supports sustainable forestry practices and contributes to a more diversified and resilient timber industry in Ghana.

WOOD RESEARCH VOLUME 69, NUMBER 4, 2024
MARIJA TODOROVIĆ, IVAN GLIŠOVIĆ, AND NADA SIMOVIĆ

EXPERIMENTAL AND NUMERICAL INVESTIGATION OF CLT PANELS WITH DIFFERENT ORIENTATIONS OF TRANSVERSE LAYERS

This paper presents an experimental and numerical investigation of two configurations of panels made of locally produced cross-laminated timber (CLT) with different orientations of laminations (boards) within transverse layers – conventional and modified orientation. Modified orientation refers to laminations of transverse layers positioned at an angle of +45° in relation to longitudinal layers. The expected advantages of modified CLT are improved mechanical performance, more efficient use of resources considering material properties, reduction in variability of characteristics within the panels and increase in shear resistance. In addition to experimental testing, numerical analysis based on finite element method was performed and successfully validated in order to serve as a more efficient tool for CLT panel investigation and optimization.

WOOD RESEARCH VOLUME 69, NUMBER 4, 2024
SINTA AMANAH, RESA MARTHA, FRIDA BASRI, MAHDI MUBAROK, ISTIE SEKARTINING RAHAYU, IRSAN ALIPRAJA, WYAN DARMAWAN, PHILIPPE GÉRARDIN, LUKAS EMMERICH, HOLGER MILITZ, AND UMMI HANI ABDULLAH

THE EFFECT OF WEATHERING ON SURFACE CHARACTERISTICS OF CHEMICALLY MODIFIED SCOTS PINE (*PINUS SYLVESTRIS*) WOOD

Scots pine (*Pinus sylvestris* L.) sapwood of 200 × 20 × 80 mm³ (L×R×T) was treated with both cell wall filling and lumen filling chemical agents (low-molecular phenol-formaldehyde, bio-oil, N-methylol/N-methyl compounds, sorbitol-citric acid, polysiloxane), which were fixed inside the wooden structure during heat-curing processes. The present study investigated the impact of the appointed chemical modifications on the surface characteristics of wood, which was addressed by measurements of the surface roughness (Ra), surface free energy (SFE), contact angles, wettability and its bonding quality. Independent of the chemical agents applied, Ra decreased as result of the chemical treatments, while SFE experienced a reduction. The Ra and SFE of both untreated and modified pine specimens increased after weathering processes. The weathering was appointed to cause a decrease in the equilibrium contact angle (θe) and an increase in the constant contact angle change rate (K-value). Increasing K-values after weathering for both untreated and modified pine specimens indicated their better wettability. Increasing wettability after weathering led to better adherence of acrylic paints on the surface of the Scots pine wood. In summary, the chemical modifications decreased the Ra and SFE of the pine sapwood, which may as a consequence affect the wettability and bonding quality of wood during outdoor exposure.

WOOD RESEARCH VOLUME 69, NUMBER 4, 2024
CHUMIN CHEN, MING LI, SAIYIN FANG, AND BO ZHANG

ANISOTROPIC VELOCITY MODEL AND ENERGY ATTENUATION CHARACTERISTICS OF ACOUSTIC EMISSION SIGNALS IN FINGER-JOINTED TIMBER AND SAWN TIMBER

Although anisotropic propagation behavior of acoustic emission (AE) in the sawn timber (ST) has been revealed, that in finger-jointed timber (FJT) is still less known. Therefore, a series of velocity and energy models of AE signals were built as it propagates along different directions on the surface and inside of specimens (ST and FJT). At first, using polar coordinate system, velocity model in 3D directions was built in FJT, which was compared to ST. Furthermore, a continuous sine wave with a frequency of 165 kHz was selected as AE source to explore the energy attenuation law in FJT and ST respectively. The results showed that there are significant differences in velocity models between FJT and ST. The wavefront in ST was regular elliptical, while that in FJT has a clear depression in perpendicular to grain direction. This feature becomes more obvious with the increase of distance when AE signal propagates inside the FJT. Inside the FJT, energy magnitude in ST was 3.00-7.37 times of that in FJT.

WOOD RESEARCH VOLUME 69, NUMBER 4, 2024
JINGE XIE, HONGHAI LIU, YU XIE, AND XIAOKAI ZHANG

INFLUENCE OF TEMPERATURE AND PRESSURE ON SUPERCRITICAL CO₂ DEWATERING OF BAMBOO STRIPS

In this study, there pressure (15, 22.5, 30 MPa) and two temperature (45, 60°C) of ScCO₂ dewatering were tested on Moso bamboo (*Phyllostachys edulis*) strips. The aim was to research the effects of these conditions on the dewatering rate, moisture distribution, and shrinkage of bamboo. The results showed that: 1) The first cycle discharges the most water of all drying conditions. The most effective dewatering time consisted of a 15 min depressurization period and a 5 min discharge period. 2) The ScCO₂ dewatering rate of bamboo strips decreased with decreasing MC, with a maximum decrease of 78%. The maximum and minimum dewatering rates were 37.04%/h and 4.41%/h, respectively. The dewatering rate was synergistically affected by temperature and pressure, which increased significantly with pressure at 45°C, but was minimized at 60°C at 22.5 MPa. 3) After dewatering, the moisture distribution in the bamboo strips shows a trend of higher moisture content (MC) in the middle and lower MC on both sides in the tangential and radial directions. 4) Most of the bamboo strips produced shrinkage after the 1st cycle of dewatering, and the overall shrinkage in the tangential direction was greater than that in the radial direction. The maximum tangential and radial shrinkage ratios are 3.06% (22.5 MPa/45°C) and 0.94% (15 MPa/60°C), respectively.

WOOD RESEARCH VOLUME 69, NUMBER 4, 2024
DOAN VAN DUONG, MASUMI HASEGAWA, MANH TUONG VU, AND VAN HUNG HOANG

RADIAL AND AMONG-CLONAL VARIATIONS OF TRANSVERSE SHRINKAGE AND BASIC DENSITY IN 5-YEAR-OLD *ACACIA AURICULIFORMIS* CLONES PLANTED IN VIETNAM

This study investigated transverse shrinkages and wood density for *Acacia auriculiformis* trees from six clones planted in north-central Vietnam. Radial and among-clonal variations of partial and total shrinkages in tangential (relative to Tn and T) and radial (relative to Rn and R) directions, partial and total coefficient of anisotropy (relative to Tn/Rn and T/R), and basic

density (BD) were examined. There were significant differences among clones for Rn and R, but no significant differences were found among clones for Tn and T. The lowest average Rn and R were detected in clones Clt38 and Clt26, suggesting that these clones might be more appropriate for breeding programs focused on improving shrinkage traits for sawn timber production. BD is not a good indicator for predicting transverse shrinkages. In contrast, stress wave velocity measured in standing trees has the potential to be used as a non-destructive method for predicting the transverse shrinkage of *A. auriculiformis* planted in Vietnam

WOOD RESEARCH VOLUME 59, NUMBER 4, 2024

LEIF PORTAL, ROGER CHAMBI, JÚLIA GIL, GABRIEL PEREIRA, AND MARIO TOMAZELLO

MAPPING WOOD DENSITY VARIATION USING QGIS: AN INNOVATIVE APPROACH FOR CHARACTERIZATION OF OCHROMA PYRAMIDALE, ACACIA MANGIUM, EUCALYPTUS GRANDIS, AND PINUS SP.

This study explores the innovative application of QGIS for mapping radial wood density variation across the entire cross-section of selected native and non-native forest species, aiming to enhance wood characterization. Using samples from *Ochroma pyramidale*, *Acacia mangium*, *Eucalyptus grandis*, and *Pinus sp.*, we applied X-ray densitometry to obtain high-resolution images, which were then analyzed with QGIS to create detailed density maps. These maps provided a clear visualization of radial density variation, offering insights into the internal structure of the wood. The integration of QGIS with X-ray densitometry proved to be an effective tool for assessing wood density variation, supporting more precise and sustainable forest management practices



Short notes

**EXPERIMENTAL STUDY ON FLEXURAL BEHAVIOR OF RED MERANTI
(*SHOREA SPP.*) GLULAM BEAM OF VARIOUS NUMBER OF LAMINAE**

YOSAFAT AJI PRANATA
UNIVERSITAS KRISTEN MARANATHA
INDONESIA

BAMBANG SURYOATMONO
UNIVERSITAS KATOLIK PARAHYANGAN
INDONESIA

(RECEIVED OCTOBER 2024)

ABSTRACT

This research aims to study flexural behavior of Red Meranti (*Shorea spp.*) glulam beam of various number of laminae by carrying out testing beams made from four, six, and eight laminae. Four points bending test method according to ASTM 198-22 was applied. The research results show that glulam composed of a smaller number of laminas reaches a smaller flexural rigidity. The empirical equations for flexural strength ratio and modulus of rupture ratio, and the trend of flexural rigidity between glulam and solid proposed in this study can be used in designing the flexural members of timber buildings, timber bridges, and in calculating the deflection of timber beams.

KEYWORDS: Flexural rigidity, flexural strength, modulus of rupture, glulam, red meranti.

INTRODUCTION

Several previous studies dedicated to establishing mechanical properties, especially flexural strength and modulus of rupture, of various wood species have been carried out, including research to study the flexural behavior of solid red Meranti wood (*Shorea spp.*) by Noh and Ahmad (2017). The flexural strength, modulus of rupture, and the flexural modulus of elasticity obtained experimentally in the study were 23.06 MPa, 56.87 MPa, and 9160.00 MPa, respectively. Baharin et al. (2020) measured the flexural strength, the modulus of rupture, and

the flexural modulus of elasticity of solid red Meranti wood at 31.83 MPa, 52.23 MPa, and 12790.55 MPa, respectively. Dayadi (2022) resulted in the modulus of rupture and the flexural modulus of elasticity of solid red Meranti wood of 76.24 MPa and 9801.36 MPa, respectively. Lee et al. (2024) obtained the modulus of rupture and flexural modulus of elasticity of red Meranti wood of 81.08 MPa and 12169.00 MPa, respectively.

Study of flexural behavior of glulam beams have also been carried out. Research on the effect of lamina thickness on the flexural strength and flexural modulus of elasticity of glulam beams was carried out by Pulngern et al. (2020). The results indicated that the lamina thickness had little effect on flexural performance of Douglas fir glulam beam.

The objective of this research is to study the flexural behavior of glulam beams made of red meranti (*Shorea spp.*). Experimental tests of such beams were performed to obtain empirical equations, namely flexural strength ratio, modulus of rupture ratio, and flexural rigidity. The term ratio herein means the ratio between the property of glulam and the property of solid beam. The scope of this research are as follows. Glulam beams are made from four laminae (90 mm x 164 mm), six laminae (90 mm x 246 mm), and eight laminae (90 mm x 328 mm), each consisting of 3 test specimens. The thickness of each lamina is 41 mm. Flexural testing uses the four points bending test according to ASTM 198-22 (2022a). Flexural rigidity (EI), flexural strength (F_b) in terms of proportional or yield load, and the modulus of rupture (MoR) were studied.

MATERIAL AND METHODS

Glulam meranti products were produced by Woodlam Indonesia. In this research, the four points bending test method was used, referring to ASTM D198: 2022 (Fig. 1). A similar test method based on the EN 408 was used in previous research to study the flexural strength and the modulus of elasticity of wood by Herda et al. (2024).

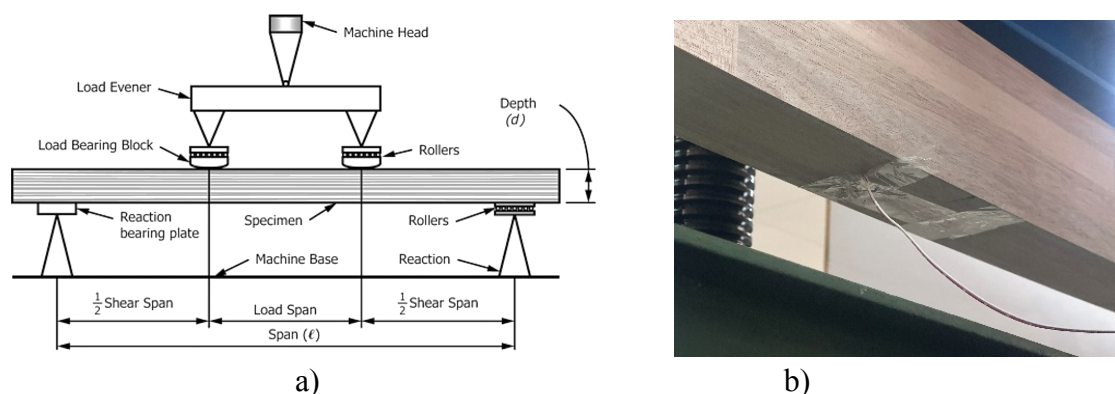


Fig. 1: a) A schematic of the bending test according to ASTM D198: 2022, b) strain gauge placed at tension surface.

Destructive experimental testing of glulam beams has been conducted with a total of 9 test specimens with total length 2000 mm and clear span 1600 mm. Tab. 1 shows the test specifications and the number of test specimens. Destructive tests were performed using Electro-hydraulic servo universal testing machine HT-9501 with maximum load capacity of

1000 kN (Hung Ta 2008). The relationship between the load obtained from the machine head and mid-span deflection of the beam were obtained for each test specimen.

Tab. 1: Specimens identity.

N ^o	Specimen ID	b (mm)	d (mm)	Number of laminae
1	BGM.90.126.1	90	164	4
2	BGM.90.126.2			
3	BGM.90.126.3			
4	BGM.90.210.1		246	6
5	BGM.90.210.2			
6	BGM.90.210.3			
7	BGM.90.294.1		328	8
8	BGM.90.294.2			
9	BGM.90.294.3			

Determining the yield point

To calculate the flexural strength, the proportional or the yield point must be determined. This point indicates when plastic deformation begins. To obtain the yield point, the Yasumura and Kawai method (Munoz 2010) was used. The first step is to calculate the initial stiffness (straight line) between 10% and 40% of the maximum load that can be obtained from the load-displacement (P-Δ) curve from the experimental tests. The second step is to connect two points with 40% and 90% of the maximum load. The third step is to calculate a tangent-line to the load-displacement curve, parallel to the 40%-90% line generated in the second step. This last line represents the post-elastic condition. The intersection between the 40%-90% line with the tangent-line was projected horizontally towards the load-displacement curve to obtain the point called yield or proportional load and displacement. This method was used to calculate the yield load (P_y) and the P-Δ curves are results of experimental tests (Pranata and Suryoatmono 2013).

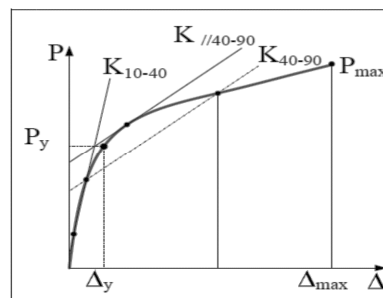


Fig. 2: Yasumura and Kawai yield point method (Munoz 2010).

Polynomial regression analysis

An assumed relationship between a response, which is dependent variable, and an input variable (in term of independent variable) implies a constant rate of change. The straight-line model involving one independent variable is the second-order polynomial or quadratic model (Rawlings et.al. 2013). The quadratic model includes the term x^2 in addition to x . This model is a case of the multiple regression model where $x_1 = x$ and $x_2 = x^2$:

$$\varepsilon_{(y)} = \beta_0 + \beta_1 \cdot x + \beta_2 \cdot x^2 \quad \text{quadratic model} \quad (1)$$

$$\varepsilon_{(y)} = \beta_0 + \beta_1 \cdot x + \beta_2 \cdot x^2 + \dots + \beta_p \cdot x^p \quad \text{polynomial model} \quad (2)$$

Higher order polynomials in Eq. 2 allow increasing flexibility of the response relationship and are cases of the multiple regression models.

RESULTS AND DISCUSSION

Fig. 3 shows the destructive experimental testing of glulam beams using four points bending test method. The tests were displacement controlled with a constant displacement speed of 2.5 mm/min. This was in accordance with ASTM D198-22 (2022a).

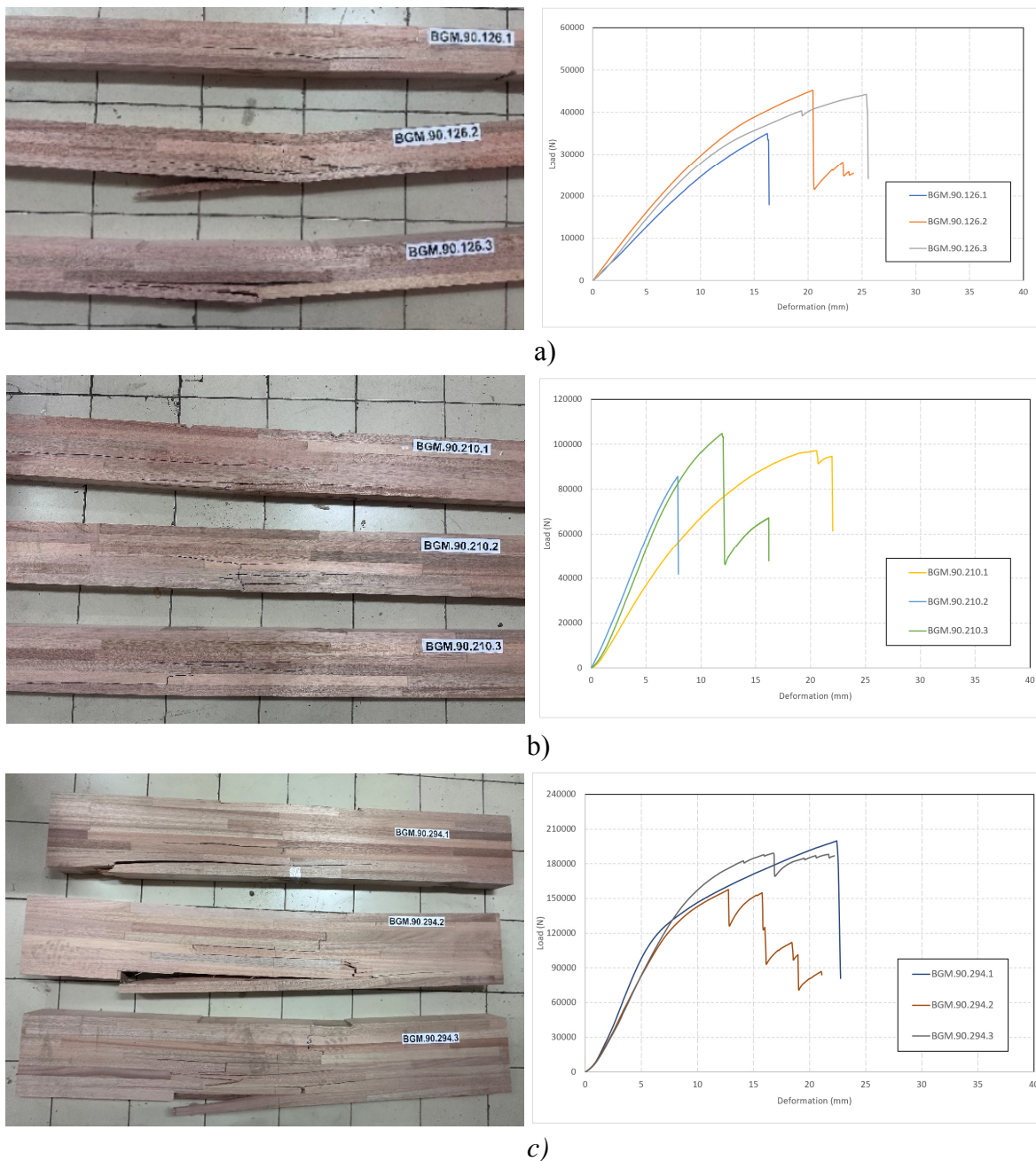


Fig. 3: The failure mode and load versus deformation relationship curve of four (a), six (b) and eight (c) laminae glulam beams.

The result of flexural strength as shown in Tab. 2 is calculated using flexure formula in beam theory (Hibbeler 2023). The flexural strength of solid wood is obtained from previous research (Baharin et.al. 2020). The modulus of rupture of solid wood is obtained from previous research as well (Lee et al. 2024). The flexural rigidity ratio is calculated using beam deflection theory (Goodno and Gere 2021). The presence of adhesive in glulam beams causes less ductile behavior compared to solid beams. This is proven by the results of the study. As seen in Tab. 2, the average displacement ductility (μ) of the tested glulam beams are quite small, namely 1.29 (glulam with four laminae), 1.16 (glulam with six laminae), and 1.56 (glulam with eight laminae). Note that one glulam specimen with eight laminae had ductility of 2.15, a value of which was much higher than the other two specimens. Therefore, if this specimen is considered as outlier, the average ductility of the other two specimens is 1.26. On the other hand, the average displacement ductility of Red Meranti solid beams is 1.56 (Pranata et al. 2011).

Tab. 2: Results of flexural strength (F_b) and modulus of rupture (MoR) of glulam beams.

Specimen	P_y (N)	P_{ult} (N)	D_y (mm)	D_{ult} (mm)	μ (mm/mm)	F_b (MPa)	MoR (MPa)
Four laminae							
BGM.90.126.1	31994.76	34959.32	15.54	16.22	1.23	36.95	40.37
BGM.90.126.2	40023.16	45183.17	15.43	20.45	1.33	46.22	52.18
BGM.90.126.3	40333.68	44196.06	19.43	25.48	1.31	46.58	51.04
Average	37450.53	41446.18	16.80	20.72	1.29	43.25	47.86
Six laminae							
BGM.90.210.1	93214.86	97131.20	17.72	20.50	1.16	38.75	40.38
BGM.90.210.2	76032.61	85613.67	7.10	8.19	1.15	31.61	35.59
BGM.90.210.3	98602.62	104762.84	10.14	11.95	1.18	40.99	43.55
Average	89283.36	95835.90	11.65	13.55	1.16	37.12	39.84
Eight laminae							
BGM.90.294.1	146595.82	199839.92	10.43	22.39	2.15	31.09	42.39
BGM.90.294.2	143954.00	157765.81	10.30	12.76	1.24	30.53	33.46
BGM.90.294.3	177334.83	189117.58	12.86	16.73	1.30	37.61	40.11
Average	155961.55	182241.10	11.20	17.29	1.56	33.08	38.65

P_y is the proportional or yield load calculated using Yasumura and Kawai method, P_{ult} is the ultimate load, D_y is the deformation at proportional or yield point, and D_{ult} is the deformation at ultimate point, μ is displacement ductility (D_u/D_y).

The glulam-to-solid ratios of F_b and MoR obtained in this study (Tab. 3) show that for beams with the same cross-sectional size made of more laminae have glulam-to-solid ratios of both F_b and MoR. This should be the case because for same cross-sectional size the more laminae glulam has, the less structural integrity it has, and therefore F_b and MoR are lower.

Tab. 3: Results of glulam-to-solid ratios of flexural strength and modulus of rupture.

Specimen	F_b (MPa)	Ratio of F_b (glulam-to-solid ratio)	MoR (MPa)	Ratio of MoR (glulam-to-solid ratio)
Solid	55.08	-	81.08	-
Glulam with four laminae	43.25	0.79	47.86	0.59
Glulam with six laminae	37.12	0.67	39.84	0.49
Glulam with eight laminae	33.08	0.60	38.65	0.48

Regarding the glulam-to-solid ratio of flexural rigidity (EI), Tab. 4, shows that for glulam beam of the same cross-sectional size with more laminae, the ratio is lower. This should be the case because glulam with more laminae has more possibility of experiencing post-elastic behavior and slip in the adhesive layers and por.

Tab. 4: Results of flexural rigidity of glulam beams.

Specimen	b (mm)	d (mm)	EI _x (solid)	EI _x (glulam)	Ratio of EI _x (glulam-to-solid)
Glulam with four laminae	90	164	403005898560	347265677707.51	0.86
Glulam with six laminae	90	246	1360144907640	1100171788734.74	0.81
Glulam with eight laminae	90	328	3224047188480	2065306548358.89	0.64

Furthermore, by using polynomial regression analysis, an empirical equation can be prepared to obtain a prediction of the ratio of flexural strength (rF_b) of glulam-to-solid with the number of lamina parameters as shown in Fig. 4a as follows:

$$rF_b = 1.088 + 0.0906.n + 0.00367.n^2 \quad R_{\text{square}} = 99,9\% \quad (3)$$

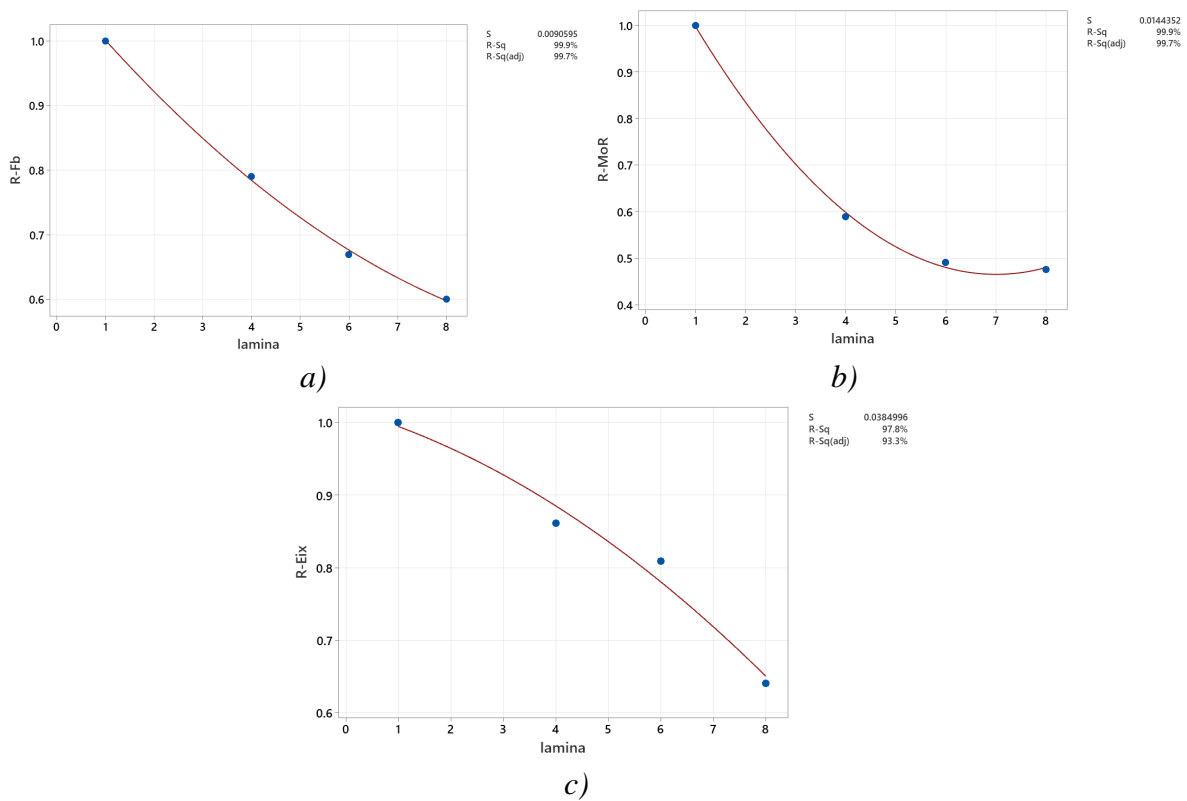


Fig. 4: Ratio of the flexural strength (a), modulus of rupture (b), and flexural rigidity (c) between glulam and solid.

In the same way, an empirical equation for the modulus of rupture ratio ($rMoR$) can be prepared as shown in Fig. 4b as follows:

$$rMoR = 1.19 + 0.207.n + 0.0148.n^2 \quad R_{\text{square}} = 99,8\% \quad (4)$$

Eqs. 3-4 can be used in design of the flexural structural components of timber buildings, timber bridges, and calculating the stiffness (deflection) of timber beams. Results obtained from Tab. 4 and Fig. 4c indicate that the flexural rigidity EI of glulam beams are not the same as solid beam. Glulam beams with smaller number of laminae produce larger glulam-to-solid ratios of flexural rigidity because they behave closer to those of solid beams.

CONCLUSIONS

The research results show that red Meranti (*Shorea spp.*) glulam beams with smaller number of laminae produces larger glulam-to-solid ratios of flexural rigidity, flexural strength and modulus of rupture. This is because the glulam beam with the smaller number of laminae is closer to the beam with solid cross-section. The proposed empirical equations for glulam-to-solid ratios of flexural strength, ratios of modulus of rupture, and flexural rigidity can be used in design of the flexural structural components of timber buildings, timber bridges, and calculating the stiffness (deflection) of timber beams. If the flexural strength of the solid beam made of Red Meranti is known, the flexural strength of the glulam beam made of Red Meranti of the same dimension (width and depth) with certain number of laminae can be estimated using the proposed equation. The other proposed equation can be used to estimate modulus of rupture of the glulam beam made of Red Meranti in a similar way.

ACKNOWLEDGMENTS

The authors gratefully acknowledge the support from Universitas Kristen Maranatha (Research: collaboration schemes with domestic partners, Fiscal Year 2022). The authors also gratefully acknowledge the support from Woodlam Indonesia and all staffs and technicians of Structures and Concrete Laboratory of Universitas Kristen Maranatha for facilitating successful experimental tests results.

REFERENCES

1. ASTM D198, 2022: Standard test methods of static tests of lumber in structural sizes.
2. ASTM D143, 2022: Standard test methods for small clear specimens of timber.
3. SNI 7973, 2013, Badan Standarisasi Nasional (in Indonesian).
4. BAHARIN, A., AHMAD, Z., CHEN, L.W., 2020: Bending strength properties of keruing and light red meranti in structural size in accordance with Eurocode 5. *International Journal of Innovative Technology and Exploring Engineering*, 9(4): 1323-1327.
5. BODIQ, J., JAYNE, B.A., 1982: *Mechanics of wood and wood composites*. Publisher New York Van Nostrand Reinhold.
6. EN 408, 2005: *Timber structures. Structural timber and glued laminated timber. Determination of some physical and mechanical properties*.

7. DAYADI, I., 2021: Effect of width, thickness, and length on static bending of red meranti (*Shorea sp.*). The 3rd International Conference on Mathematics and Sciences, AIP Conference Proceeding 2668, pp. 060002-1–060002-5.
8. GOODNO, B.J., GERE, J.M. 2021: Mechanics of Materials 9th Edition. pp. 480-512.
9. HERDA, R., SLIVANSKY, M., BRODNIANSKY, J., KLAS, T., 2024: Determination of flexural strength and young's modulus of elasticity of actively bent wood. Wood Research 69(3): 485-494.
10. HIBBELER, R.C., 2023: Mechanics of Materials, 11th edition. pp. 512-568.
11. HUNG TA, CO., LTD., 2008: HT-9501 Electro-Hydraulic Servo Universal Testing Machines, year of production 2008, Hung Ta Instrument (Thailand) Co., Ltd., Bangplee, Samutprakarn 10540.
12. LEE, M.D., TANG, R.W.C., MICHAEL, Z., KHAIRULMAINI, M., ROSLAN, A., KHODORI, A.F., SHARUDIN, H., LEE, P.S. 2024: Physical and mechanical properties of light red meranti treated with boron preservatives. Journal of the Korean Wood Science and Technology, 52(2): 157-174.
13. MUNOZ, W., MOHAMMAD, M., SALENIKOVICH, A., QUENNEVILLE, P., 2010: Determination of yield point and ductility of timber assemblies: In Search for a Harmonized Approach, Engineered Wood Products Association.
14. NOH, N.I.F.M., AHMAD, Z., 2017: Heat treatment on keruing and light red meranti: The effect of heat exposure at different levels of temperature on bending strength properties, IOP Conference Series: Materials Science and Engineering 271: 012060.
15. PRANATA, Y.A., SURYOATMONO, B. 2013: Nonlinear finite elemen modeling of red meranti compression at an angle to the grain, Journal of Engineering and Technological Science, Volume 45 No. 3, pp. 222-240.
16. PRANATA, Y.A., SURYOATMONO, B., TJONDRO, J.A. 2011: Numerical and experimental research of flexural strength of Indonesian timber (*in indonesian*), proceeding of national conference I BMPTTSSI - KoNTekS5, pp. 143-150, University of North Sumatera, Medan, Indonesia, 14 October 2011.
17. PULNGERN, T., CHANTO, K., PANSUWAN, W., 2020: Effect of lamina thickness on flexural performance and creep behavior of Douglas fir glued laminated timber beam. Wood Research 65(5): pp. 715-726.
18. RAWLINGS, J.O., PANTULA, S.G., DICKEY, D.A., 2013: Applied regression analysis, A research tool, 2nd Ed., Springer New York, NY. pp. 235-268.

YOSAFAT AJI PRANATA*
UNIVERSITAS KRISTEN MARANATHA
FACULTY OF SMART TECHNOLOGY AND ENGINEERING
JL. SURIA SUMANTRI 65, BANDUNG, 40164
WEST JAVA, INDONESIA

*Corresponding author: yosafat.ap@gmail.com

BAMBANG SURYOATMONO
UNIVERSITAS KATOLIK PARAHYANGAN
FACULTY OF ENGINEERING
JL. CIUMBULEUIT 94, BANDUNG, 40161
WEST JAVA, INDONESIA